A Model of Desertification Process in a Semi-arid Environment Employing Multi-spectral Images

Jorge Lira

Instituto de Geofísica-UNAM,
Circuito Institutos, Cd. Universitaria
04510 México DF, México
lira@geofisica.unam.mx

Abstract. A model of desertification in semi-arid environment employing satellite multi-spectral images is presented. The variables proposed to characterize desertification are: texture of terrain, vegetation index for semi-arid terrain, and albedo of terrain. The texture is derived from a divergence operator applied upon the vector field formed by the first three principal components of the image. The vegetation index selected is the TSAVI, suitable for semi-arid environment where vegetation is scarce. The albedo is calculated from the first principal component obtained from the bands of the multi-spectral image. These three variables are input into a clustering algorithm resulting in six desertification grades. These grades are ordered from no-desertification to severe desertification. Details are provided for the computer calculation of the desertification variables, and the parameters employed in the clustering algorithm. A multi-spectral Landsat TM image is selected for this research. A thematic map of desertification is then generated with the support of ancillary data related to the study area.

1 Introduction

The process of desertification is affecting large areas of the Earth surface with social and economic consequences. There is no consensus on a definition of desertification applicable in all regions and accepted by researchers of all concerned disciplines. Hence, a model that quantifies the surface manifestations of desertification from the remote sensing point of view may help to understand such definition. In addition to this, a model is useful to derive quantitative conclusions, such as: i) to determine the degree and extension of desertification, ii) to monitor the desertification over the years, and iii) to simulate various scenarios of desertification.

The causes of desertification are divided in two broad categories: natural and anthropogenic. A climate change producing dry atmospheric conditions brings drought leading to a decline in biological productivity. The origin of anthropogenic causes is related to cultivation practices, rangeland use, and fire ignition of vegetation species. The origin of natural causes is climate change, whether long term or indefinite. Both, the climate and the anthropogenic causes produce a reduction of the quantity and diversity of natural vegetation [1], [2], [3], [4]. In addition to this, the consequences

A. Sanfeliu et al. (Eds.): CIARP 2004, LNCS 3287, pp. 249–258, 2004.

of climate change and anthropogenic activities upon soil and vegetation degradation, and upon erosion processes, may be observed by means of satellite data [5], [6], [7]. The main ecological conditions characterizing desertification may be resumed as follows: increase of aridity, irregular but intense precipitation leading to irregular runoff, extreme events such as droughts causing soil erosion, desiccation and salinization of soils, and decline of vegetation. The main physical aspects characterizing desertification are: displacement of desert-like conditions, change of vegetation cover types, change of vegetation density, increase in albedo, and smoothness of terrain roughness.

In one of the earliest works related to desertification, Robinove and co-workers [8] uses differencing registered images of albedo to measure general conditions of an arid land. These workers determined that albedo is correlated with: erosion, increases or decreases in soil moisture, and increases or decreases in vegetation density. They concluded that decrease of albedo implies an improvement of land quality, and that increase of albedo implies a degradation of land quality. Albedo is therefore an indicator to measure desert-like conditions. In brief, in desertification processes, a change of vegetation cover types and a change of vegetation density results in an increase of albedo due to the exposure of soil.

Desertification results in changes of the quantity and composition of vegetation: a vegetation dynamics that results in a decline of plant cover and biological productivity [9], [10]. On the other hand, semi-arid areas comprise a series of vegetation complexes with various canopy closures over a variety of soils. To measure the vegetation dynamics in desertification processes for semi-arid environments a number of authors have used vegetation indices [10], [11].

Ecological circumstances and anthropogenic activities combine to generate conditions of physical land degradation. This leads to a change of texture of terrain surface, the stronger the desertification the smoothness the texture [12]. Non-desertified areas show homogeneous vegetation cover with a certain texture. When a desertification process develops, low-variability areas are decreased and replaced by higher variance areas [13]. Hence, environmental heterogeneity increases as a result of desertification processes. Increased spatial heterogeneity is an indicator of desertification [14]. As the desertification further proceeds, the spatial heterogeneity decreases reaching a limit - in desert-like conditions - when terrain surface appears smooth. From space, spatial heterogeneity may be observed as terrain texture. Therefore, under desertification processes, texture varies from a certain roughness to the limit, in desert-like conditions, when texture is smooth.

On the grounds of the above discussion, three variables may be considered to characterize desertification processes from the remote sensing standpoint: albedo of terrain, vegetation strength, and terrain texture. These variables have been considered independently by previous works, however, they must be considered concurrently to provide full, quantitative description of desertification conditions. Based on the above discussion, the following objectives are set: i) to define the variables that characterize desertification processes from a remote sensing view point, ii) to establish a model based on these variables, and iii) to produce a thematic map of desertification strength in semi-arid environment.

2 Area Description, Methods and Materials

2.1 Study Site

An area of northern Mexico, where semi-arid conditions prevail, was selected to test the desertification model proposed in this research. From the Landsat image given by path/row = 29/41, a sub image was extracted from certain pixel coordinates. This sub image is geocoded to UTM projection with a pixels size of 28.5 x 28.5 m^2. The size of this sub image is: 1700 pixels x 2048 lines. The acquisition date is: July 29, 1996. The geographic coordinates are: northwest corner: 27° 30′ 39.36″ W, 101° 39′ 33.36” N, southeast corner: 26° 59′ 34.22″ W, 101° 9′ 32.47″ N.

The elevation in this area ranges between 450 and 1400 meters above sea level. Sedimentary rocks form the dominant lithologic unit of the area. The climatic conditions prevailing for till-plains and high lands, for elevations ranging between 1,000 and 1400 meters, determine a dry and semi-dry atmosphere. In areas with till-plains and hills, for elevations ranging between 500 y 1000 meters, the climatic conditions are warm temperatures and dry atmosphere. The predominant climate types are BSohw and BS1kw, semiarid temperate [15]. The average annual temperature is 22° C. The annual average precipitation is between 300 and 400 mm.

Climatological conditions prevailing in the area support the presence of a widely spread halophilous vegetation in the highs of the mountains. Areas with shrubbery, grass/herbage and agriculture fields are present in plains and till-plains. Other areas with soil and soil/herbage correspond to zones of exposed soil with a certain degree of erosion and spare vegetation. Overgrazing, pasture, and agriculture not suited for the area occur as well. Natural conditions determine a dry temperate climate with low precipitation, whereas anthropogenic activities impose stressing conditions to vegetation cover types. These two conditions are driving the selected study area towards a desertification process.

2.2 Desertification from Space

Viewed from space, desertification manifests itself as variations of spatial heterogeneity, vegetation strength and albedo. As the desertification process develops, the spatial heterogeneity of the spectral cover types varies from a certain value up to some maximum of spatial heterogeneity. If the desertification further proceeds, the number of cover types diminishes leading to a scene of homogeneous appearance. Spatial heterogeneity varies from a certain roughness up to a certain maximum value diminishing consecutively to smooth roughness. On the other hand, the albedo of the scene increases from some value up to a maximum when vegetation is scarce or nil. In addition to this, salinization of the soil further increases the value of albedo. When biological productivity is completely lost in a certain area, vegetation cover types are absent so the soil is fully exposed leading to high values of albedo. Furthermore, the density and strength of vegetation decreases as desertification processes develops. Therefore, we propose that desertification, as observed from space, can be modeled by measurement of three variables: texture, albedo and vegetation strength. None of these variables by themselves can account to characterize the strength and variability

of desertification. These variables must be taken concurrently, measured from the same image, and used to describe the spatial distribution of desertification in a given area. The set of such variables may be used to write an expansion of the image to describe desertification processes; details of this are given in the next section.

Desertification is a process that may take a long time to develop. To study in time such process, a series of images of the same scene for different dates would be required. The analysis of many images for a long period is costly and time consuming. Therefore, ergodicity must be assumed. Physically, ergodicity is satisfied whenever the observation, in different times, of n-copies of a system is equivalent to the observation in time of a single system. This means that from a single image different stages of desertification may be observed. The image must cover an area embracing a set of zones where desertification is present in different stages of development. In the present research, it is sufficient to assume ergodicity with respect to the first two statistical moments: the mean and the autocorrelation. To satisfy this statistical condition, the random field formed by the three variables characterizing desertification processes must be stationary or homogeneous. On the other hand, published research reveals the existence of a second order stationarity of the data used to study desertification processes [13]. In addition to this, second order stationarity implies the ergodicity for the first two statistical moments [16]. On the grounds of these results, ergodicity for the mean and autocorrelation is assumed. This assumption is sufficient for the purposes of this research, i.e., preparing a thematic map where several levels of desertification strength may be appreciated from a single image.

2.3 Desertification Model

A representation of a multi-spectral image **g** is expressed by the following equation

$$g_i(k,l) = \mu_i^g + \sum_{j=1}^{m} a_{ij} X_j(k,l), \ \forall\ i = 1, 2, \ldots n, \text{ and } k, l = 1, 2, \ldots M, N. \qquad (1)$$

The vector $\boldsymbol{\mu}^{\mathbf{g}} = \{ \mu_1^g, \mu_2^g, \ldots \mu_n^g \}$ represents the mean of the multi-spectral image $\mathbf{g} = \{g_1, g_2, \ldots g_n\}$ composed by n bands. The size of the image is M x N pixels. The bi-dimensional functions $X_1, X_2, \ldots X_m$, with $m \leq n$, are zero-mean random variables with a certain correlation among them. When the set of X_j are zero-mean non-correlated random functions, they are named canonical bands in terms of which the image **g** is represented [17]. The variables X_i are named the functions. The quantities a_{ij} are deterministic functions named the coeficientes. The indices (k,l) are the coordinates of a pixel in the image. When zero-mean random functions are used in equation (1), useful representation of the image **g** may follow; even when some correlation may exists among the functions X_i [17]. Hence, a suitable set of X_i variables shall represent the key factors that provide a characterization of desertification. The variables X_1, X_2 and X_3 are in general not zero-mean; therefore the mean must be subtracted.

On the grounds of the discussion provided in section one and section 2.2, the following bands to model desertification processes are proposed: X_1 - First desertifica-

tion band: albedo; X_2 - Second desertification band: texture:X_3 - Third desertification band: vegetation index.

In the present research, the functions a_{ij} are set to one; however, these functions may be used to introduce different weights to the X_i. The bands X_1, X_2 and X_3 are the variables that characterize desertification processes from the remote sensing standpoint. In this sense, a multi-spectral image is expanded in terms of the variables: albedo, texture and vegetation strength. This expansion allows the characterization of desertification processes from the remote sensing standpoint. The following section shows the necessary background to compute these variables.

2.4 Calculation of Desertification Bands

Albedo is an indicator of desertification condition. Albedo is defined as the ratio: total scattered power/incident power, integrated over the wavelength range of the multi-spectral image. On the other hand, the first principal component is directly proportional to the albedo of the cover types of terrain [18]. Therefore, to calculate the albedo, the principal components decomposition was applied to the bands of the multi-spectral image; the infrared band was not included due to a different pixel size. Hence, the first principal component is the first desertification band.

Texture is defined as a spatial organization of pixels in a certain region of the image and is directly associated to the roughness of terrain [19]. Desertification processes transform the roughness of landscape terrain. The calculation of texture is based on a vector field model for the multi-spectral image. The vector field is constructed in an n-dimensional space defined by the ensemble of multi-spectral image bands. The pixels form the vectors of this field. Upon this field, a divergence operator is applied to produce a map of texture variation in the image. The vector field flux derived by the divergence operator is directly related to terrain texture [20]. Hence, the divergence operator upon the image produces the second desertification band.

Vegetation cover types change both in density and in diversity as a consequence of desertification processes. To quantify vegetation change in semiarid environments a proper vegetation index must be used. The transformed soil adjusted vegetation index (TSAVI) shows a good behaviour to account for vegetation changes for such environments [21]. The TSAVI takes into account the reflectivity of soils that may be exposed in a semi-arid land. Hence, the TSAVI is the third desertification band. Figure 1 show a color composite of desertification bands. To complete the computation of desertification bands, and taking into account that $a_{ij} = 1$ for all desertification bands in equation (1), a linear stretch was applied to cover the range of: [0 – 255].

2.5 Classification of Desertification Bands

To prepare a thematic map of desertification grades, a non-supervised classification was applied to X_1, X_2 and X_3. The algorithm selected for this task is the ISODATA clustering procedure. The parameters used in this algorithm are the default values of the PCI Geomatica module. On the grounds of field data consisting of topographic,

vegetation and soil maps, six grades of desertification were established. The resulting classification was edited to merge clusters into one desertification grade. Depending on variations of topography, soil and vegetation, one or more clusters were needed to form one desertification grade class. The merging of clusters was done using the field data and table 1 as a general rationale to define desertification grades.

Table 1. General conditions of study site for desertification grades

Grade	Texture roughness	Albedo	Vegetation density	Topography
Nil	Various	Very low	Very high	Various elevations
Minimum	Various	Low	High	Various elevations
Low	Medium	Medium	Medium	Till-plains and low lands
Medium	Smooth	High	Low	Till plains and low lands
High	Smooth	High	Very low	Low lands
Very High	Very smooth	Very high	Soil fully exposed	Low lands

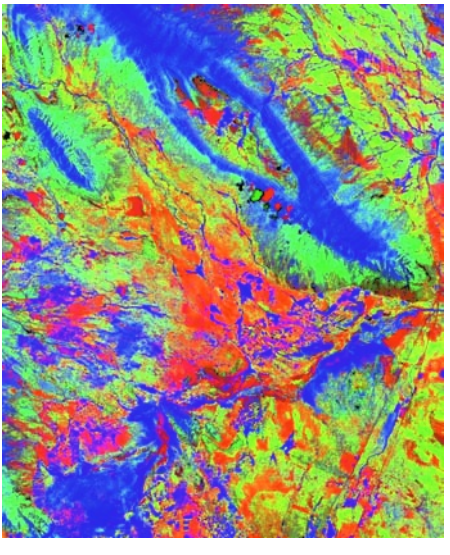

Fig. 1. Color composite of desertification bands: [RGB] = [Albedo, Texture, TSAVI]

3 Results and Analysis

The thematic map depicting six grades of desertification is shown in figure 2. There is no quantitative definition of desertification grades; therefore, on the grounds of a comparison of field data with results shown in the thematic map (Table 1), the following classification is adopted: Nil desertification – No disturbance of vegetation is appreciated. Minimum desertification – Some disturbance of vegetation is observed.

Low desertification – Moderate disturbance of vegetation is present. Medium desertification – Vegetation partially covers the soil. High desertification – Scarce vegetation is observed, soil is partially exposed. Very high desertification – No vegetation is observed, soil is fully exposed.

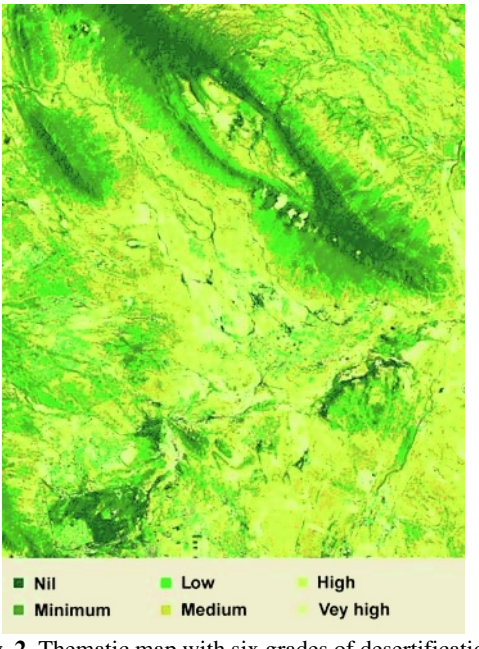

Fig. 2. Thematic map with six grades of desertification

As a rule in the above classification, the albedo steadily increases as desertification strength increases. On other hand, vegetation density strength diminishes as desertification strength increases. None the less, various texture roughnesses may be present in nil, minimum and low desertification grades. This is particularly true for agriculture fields where texture is smooth. However, medium, high and very high desertification grades always occur in areas of smooth or very smooth texture roughness. This means that vegetation density and albedo may contribute more to the determination of desertification grades. This might lead to the conclusion that different weights in equation (1) may be needed for the variables characterizing desertification processes. The ensuing discussion confirms this asseveration. Digital counts observed in desertification bands, for a selected area, confirm the above classification rationale (Table 2). An explanation of the general conditions where these grades take place follows.

Nil desertification occurs in high lands where vegetation is dense and unaltered, and texture is rough. However, this desertification grade may occur as well in low lands in areas of dense vegetation with smooth roughness; this is the case of fully developed agriculture fields (Table 3). In both situations, the albedo values are very low.

Table 2. Digital counts for nil, medium, and very high desertification grades

Desertification grade	Albedo	Texture	TSAVI
Nil	0 – 25	180 – 255	233 – 255
Medium	74 – 133	23 – 144	90 – 166
Very high	240 – 255	0 – 24	0 – 24

Table 3. Various desertification levels for selected spots

Coordinates	Altitude (m)	Vegetation	Grade
27°31' N, 101°31' W	1,050	Shrubbery, high density	Nil
27°26' N, 101°42' W	750	Shrubbery, low density	Low
27°20' N, 101°33' W	550	Grass/herbage	High
27°12' N, 101°21' W	550	Agriculture, medium density	Low
27°14' N, 101°32' W	500	Exposed soil	Very high
27°09' N, 101°11' W	500	Agriculture, high density	Nil

Minimum desertification is present in medium elevation lands with high-density vegetation and low albedo values. In this grade, the vegetation presents some disturbance: this disturbance appears as terrain areas containing some patches with low-density vegetation. None the less, this desertification grade may occur as well in low lands, in particular, for well developed agriculture fields (Table 3). Texture roughness may be medium for high elevation lands and till-plains.

A low desertification grade is associated to areas with emerging agriculture fields. This desertification grade occurs as well in till-plains with moderate disturbance of vegetation and medium albedo values. Areas of moderate disturbance of vegetation show a homogenous distribution of patches with low-density vegetation.

A medium desertification grade is associated to low vegetation density and high albedo values. The texture in this grade is always smooth. These desertification grades always occur in low lands and till-plains.

High desertification is observed in very low-density vegetation where soil is partially exposed. The texture is smooth or very smooth and albedo values are high due to the contribution of soil to the reflectance of terrain. These desertification grades always occur in low lands.

Very high desertification grade is present when vegetation is absent and highly reflected soil is fully exposed. The medium, high and very high desertification grades always take place in low lands with smooth texture roughness. The very high desertification grade is always associated to very high albedo values. These desertification grades always occur in low lands. In addition to the above, some scattered clouds are visible in the upper right quadrant of the image. As expected, clouds produce a very high desertification grade; this is a confirmation of the desertification model. On the other hand, cloud shadows modify the desertification grade on the ground.

Ergodicity is an important element in the interpretation of the desertification map. Under this assumption, the evolution of desertification may be observed in a single image. The conditions for this evolution can also be drawn as well from the desertification model. The evolution to high grades of desertification implies the smoothing of terrain jointly followed by a decrease in vegetation strength and exposure of soil. An

increase of albedo is also involved in this evolution. From a single image, it is possible to appreciate the spatial and spectral change experienced by an ecosystem when drifting from one desertification grade to some other grade. General conditions when this evolution takes place are shown in table 3. In this framework, it is expected that, in desertification processes, an area of a certain desertification grade may drift to a higher grade when natural and anthropogenic forces are set for this change.

4 Conclusion

A desertification model to describe desertification processes in a semi-arid environment from the remote sensing standpoint has been established. This model is written as an expansion of a multi-spectral image in terms of a number of bands named desertification bands. These bands represent a set of variables that characterize desertification processes in a semi-arid environment: texture roughness of terrain, vegetation density strength, and albedo of terrain surface. The model expressed in equation (1) allows the introduction of a set of coefficients a_{ij}. These coefficients may be used as weighting factors to provide different weights to each desertification band. The assumption of ergodicity in desertification processes permits the observation of the evolution from nil desertification to a high desertification grade from a single image. In addition to this, with a set of images in different times, a time series of the spatial evolution of desertification classes may be prepared. Even though the classification of desertification grades provided in this work is qualitative, digital counts in desertification bands may help to quantify these grades. Human made areas such as agriculture fields may show low or nil desertification grades even though the texture is smooth. This might lead to the conclusion that the variables X_i do not equally contribute to the characterization of desertification. However, agriculture fields are not natural spectral objects in a scene. None the less, the model proposed in this research produces a low or nil desertification grades for fully developed agriculture fields, as expected, since the biological productivity is maintained in this case.

References

1. Fredrickson, E., Havstad, K.M., Estell, R., Hyder, P.: Perspectives on Desertification: South-Western United States. J. of Arid Env. 39 (1998) 191–207
2. Rubio, J.L., Bochet, E.: Desertification Indicators as Diagnosis Criteria for Desertification Risk Assesment in Europe. J. of Arid Env. 39 (1998) 111–120
3. Puigdefábregas, J., Mendizabal, T.: Perspectives on Desertification: Western Mediterranean. J. of Arid Env. 39 (1998) 209–224
4. Barth, H.J.: Desertification in the Eastern Province of Saudi Arabia. J. of Arid Env. 43 (1999) 399-410
5. Hill, J., Sommer, S., Mehl, W., Megier, J.: Use of Earth Observation Satellite for Land Degradation Mapping and Monitoring in Mediterranean Ecosystems: Towards a Satellite-Observatory. Environ. Monitor. and Asses. 37 (1995) 143-158
6. Grigorev, A.A., Kondratev, K.Y.: Satellite Monitoring of Natural and Anthropogenic Disasters. Earth Observ. and Rem. Sens. 14 (1997) 433-448

7. Witt, R.G.: GIS and Remote Sensing Applications for Environmental Assesment. Earth Observ. and Rem. Sens. 16 (2000) 179-192
8. Robinove, C.J., Chavez, P.S., Gehring, D., Holmgren, R.: Arid Land Monitoring Using Landsat Albedo Difference Images. Rem. Sens. of Env. 11 (1981) 133-156
9. de Soyza, A.G., Whitford, W.G., Herrick, J.E., Van Zee, J.W., Havstad, K.M..: Early Warning Indicators of Desertification: Examples of Tests in the Chihuahuan Desert. J. of Arid Env. 39 (1988) 101-112
10. Xu, X.K., Lin, Z.H., Li, J.P., Zeng, Q.C.: Temporal-Spatial Characteristics of Vegetation Cover and Desertification of China Using Remote Sensing Data. Progr. in Nat. Sci. 12 (2002) 45-49
11. Palmer, A.R., van Rooyen, A.F.: Detecting Vegetation Change in the Southern Kalahari Using Landsat TM Data. J. of Arid Env. 39 (1998) 143-153
12. Tripathy, G.K., Ghosh, T.K., Shah, S.D.: Monitoring Desertification Process in Kamataka State of India Using Multi-Temporal Remote Sensing and Ancillary Information Using GIS. Inter. J. of Rem. Sens. 17 1996) 2243-2257
13. Seixas, J.: Assesing Heterogeneity From Remote Sensing Images: The Case of Desertification in Southern Portugal. Inter. J. of Rem. Sens. 21 (2000) 2645-2663
14. Schlesinger, W.H., Raikes, J.A., Hartley, A.E., Cross, A.F.: On the Spatial Patterns of Soil Nutrients in Desert Ecosystems. Ecology 77 (1996) 364-374
15. García, E.: Modificaciones al Sistema de Clasificación Climática de Kopen, Para Adaptarlo a las Condiciones de la República Mexicana. Reporte Técnico, Universidad Nacional Autónoma de México, México.
16. Papoulis, A.: Probability, Random Variables, and Stochastic Processes. McGraw-Hill, Boston (1991)
17. Dougherty, E.R.: Random Processes for Image and Signal Processing. SPIE/IEEE Press, Bellingham (1999)
18. Galvão, L.S., Vitorello, I., Paradella, W.R.: Spectroradiometric Discrimination of Laterites With Principal Components Analysis and Additive Modelling. Rem. Sens. of Env. 53 (1995) 70-75
19. Lira, J., Frulla, L.: An Automated Region Growing Algorithm for Segmentation of Texture Regions in SAR Images. Inter. J. of Rem. Sens. 19 (1998) 3595-3606
20. Lira, J.: A Divergence Operator to Segment Urban Texture. IEEE/ISPRS Joint Workshop on Remote Sensing and Data Fusion Over Urban Areas (2001) 159-163. November 8-9, Rome.
21. Baret, F., Guyot, G.: Potentials and Limits of Vegetation Indices for LAI and APAR Assesment. Rem. Sens. of Env. 39 (1991) 161-173